JAAS

PAPER

Cite this: *J. Anal. At. Spectrom.*, 2015, **30**, 353

Isotopic composition analysis of dissolved mercury in seawater with purge and trap preconcentration and a modified Hg introduction device for MC-ICP-MS

Haiying Lin,[a] Dongxing Yuan,*[a] Bingyan Lu,[a] Shuyuan Huang,[a] Lumin Sun,[b] Fan Zhang[a] and Yaqin Gao[a]

This study aimed to solve the common problems in Hg isotope analysis of water samples at low concentration. The isotope composition of dissolved Hg in seawater is reported for the first time. A modified device for introducing Hg into a multi-collector inductively coupled plasma mass spectrometer and a preconcentration method for the preconcentration of dissolved Hg were developed to enhance the sensitivity of the isotopic composition analysis method. The modified cold-vapor generator was used to transfer dissolved Hg^{2+} from the matrix into gaseous Hg^0. The purge and trap method was developed and employed to preconcentrate dissolved Hg in water samples. Keeping other parameters the same, the Hg signal generated with the modified Hg introduction device was twice as much as the commercial one (HGX 200). In the measurement of NIST SRM 3133, the external precision for δ^{202}Hg was 0.06‰ (2SD, $n = 310$), and the δ^{202}Hg value of the UM-Almadén in-house secondary standard was -0.57 ± 0.10‰ (2SD, $n = 49$), indicating that the modified device was stable and reliable. Factors influencing the efficiency of the purge and trap method, *e.g.*, concentration of $KMnO_4$ in the trapping solution, flow rate of the purge gas and purge time, were optimized. With ultrapure water (blank) and seawater (matrix) spiked with NIST SRM 3133 at Hg concentrations of 5.00–35.50 ng L^{-1} and 10.00–35.50 ng L^{-1}, the δ^{202}Hg values of the blank spike and matrix spike were 0.00 ± 0.04‰ (2SD, $n = 19$) and -0.02 ± 0.04‰ (2SD, $n = 12$), respectively. The results indicated that the purge and trap method was free from matrix interference. The results of this practical application showed good stability and reproducibility of the proposed methods.

Received 22nd July 2014
Accepted 20th October 2014

DOI: 10.1039/c4ja00242c

www.rsc.org/jaas

Introduction

Mercury (Hg) is a toxic metal of global concern.[1] Hg is released to the environment through both natural and anthropogenic pathways. Once emitted to the atmosphere, gaseous elemental Hg^0 can be transformed to reactive bivalent and particulate Hg species which can be deposited into aquatic reservoirs *via* dry and wet deposition.[2] Hg exists in the ocean mainly in inorganic forms such as dissolved Hg (Hg^0, Hg^{2+}) and particulate Hg^{2+}. Dissolved Hg may either return to the atmosphere through air–sea exchange,[3] or attach onto particulates and thus remain in seawater.

The isotopic tracing technique is an effective method in the research of Hg pollution. Using the technique, researchers have studied the source, pathway and fate of Hg in the environment, including its transport, transformation and sink. Fractionations of Hg isotopes (^{196}Hg, ^{198}Hg, ^{199}Hg, ^{200}Hg, ^{201}Hg, ^{202}Hg and ^{204}Hg) have been induced with some natural processes, *e.g.*, photo-reduction,[4] volatilization or evaporation,[5,6] and biological processes.[7,8] Previous studies report very large variations in both mass dependent fractionation (MDF) and mass independent fractionation (MIF) in solid samples, such as coals/soils,[9] sediments,[10,11] rocks,[12] hydrothermal ores,[13] biological samples,[14–16] and atmospheric precipitation.[17] The study of Hg fractionation in water samples has increased in recent years. Wang *et al.* investigated the Hg fractionation of photoreduction in natural water[18] and volatilization of Hg^0 from solution into the gas phase,[6] observing that MDF and MIF result from the preferential photoreduction and volatilization of light or odd isotopes. Sherman *et al.*[19] proved that the Hg in Arctic snow is fractionated by the re-emission of Hg^0 and sunlight-induced reactions. The MIF of even isotope ^{200}Hg is found in rain and snow samples.[20] However, few Hg isotope data [21] for seawater have been reported due to the complicated matrix and low concentration.

[a]*State Key Laboratory of Marine Environmental Science, College of the Environment and Ecology, Xiamen University, Xiamen, 361102, China. E-mail: yuandx@xmu.edu.cn; Tel: +86 5922184820*

[b]*Tan Kah Kee College, Xiamen University, Zhangzhou, 363105, China*

A multi-collector inductively coupled plasma mass spectrometer (MC-ICP-MS) is usually used to accurately analyse isotopes with a mass of 7–238. With the development of MC-ICP-MS, there is increasing interest in applying the Hg isotope tracing technique to understand the sources and behaviour of Hg in the environment. The commercial cold-vapor generator (CVG; HGX 200, CETAC, U.S.) is a commonly used sample introduction device to transfer dissolved Hg^{2+} to gaseous Hg^0,[22–24] within which the special U-shaped gas–liquid separator (GLS) has a large dead volume. A large amount of carrier gas (6–8 L min^{-1}) is needed in the device. Therefore, Hg^0 concentration is diluted by the carrier gas, which decreases signal intensity.

The concentration of Hg in water is usually as low as ng L^{-1}.[2,25,30] On the other hand, for better precision and accuracy, the isotopic analysis method needs Hg concentration in the prepared samples (samples ready for instrumental analysis) at the ng mL^{-1} level.[10,11,17,23,27,37] Preconcentration is one way to reach higher concentrations. Until now, two methods have been successfully performed in preconcentrating Hg in water samples. The gas–liquid separation and trap method[17,19,26] employs a GLS to separate Hg^0 from the samples, and then trap Hg^0 in $KMnO_4$ solution. Alternatively, AG 1 × 4 ion-exchange resin is used to directly preconcentrate Hg from freshwater [26] and seawater.[21] Although the two methods have resulted in quantitative yields and been applied to analysing Hg isotopes in natural waters, they suffer some disadvantages. For instance, the gas–liquid separation method consumes much more reagent during the reduction process, and it usually takes a long time to treat liters of water at the introduction rate of 0.8 mL min^{-1}.[17] Even more, the enrichment factor is limited with the gas–liquid separation method. The preconcentration process with the ion-exchange resin has to be carried out in a clean room to avoid possible contamination.

A refined two-stage gold amalgamation preconcentration technique[24,28] has been applied for the determination of Hg in seawater at sub-ng L^{-1} with recovery higher than 95%. It takes 30 min to purge Hg from 500 mL of seawater.[28] The Au column used in the method for absorbing gaseous Hg^0 is easily purified with less contamination. ^{204}Hg has significant isobaric interference ^{204}Pb; the commonly used procedure to eliminate isobaric interference is mathematical correction following an appropriately designed algorithm.[29,31] With the gold amalgamation preconcentration technique, Hg can be completely separated from Pb, thus precise determination of ^{204}Hg composition without correction can be achieved. Since the sample state is required to be liquid before introduction to the MC-ICP-MS, Hg preconcentrated on the Au column has to be transferred into solution. $KMnO_4$ solution is commonly used[17,20,26] for oxidizing and trapping Hg^0.

The purge and trap method is practical and free from seawater with high salt matrix. For the measurement of the dissolved Hg isotope composition in seawater, a modified CVG Hg introduction device and a purge and trap preconcentration method with gold amalgamation and $KMnO_4$ solution trapping were developed in this study. Application of the method to the analysis of dissolved Hg isotopic composition in seawater was carried out.

Materials and methods

Instrumentation and measurement

The Hg isotope analysis system can be divided into two parts, the introduction device and the analysis/detection instrument. As shown in Fig. 1, the introduction device included a modified CVG for Hg introduction and a desolvating nebulizer (DSN-100, Nu Instruments, Great Britain) for thallium (Tl) introduction. MC-ICP-MS (Nu Plasma HR, Nu Instruments, Great Britain) was employed as the analysis/detection instrument. The modified CVG was made out of a self-designed quartz tube, in which Hg standard or sample solutions were adequately mixed with tin chloride ($SnCl_2$) in a tee junction (t1), and pumped into the GLS from the top. The Hg^0 in the mix solution was blown off with a counter-flow argon (Ar) gas at flow rate of 80–100 mL min^{-1} from the bottom of the GLS. After removing moisture in the carrier gas with a 0.45 μm PTFE filter, Hg^0 was mixed with the Tl aerosol and injected into the ICP. Two peristaltic pumps

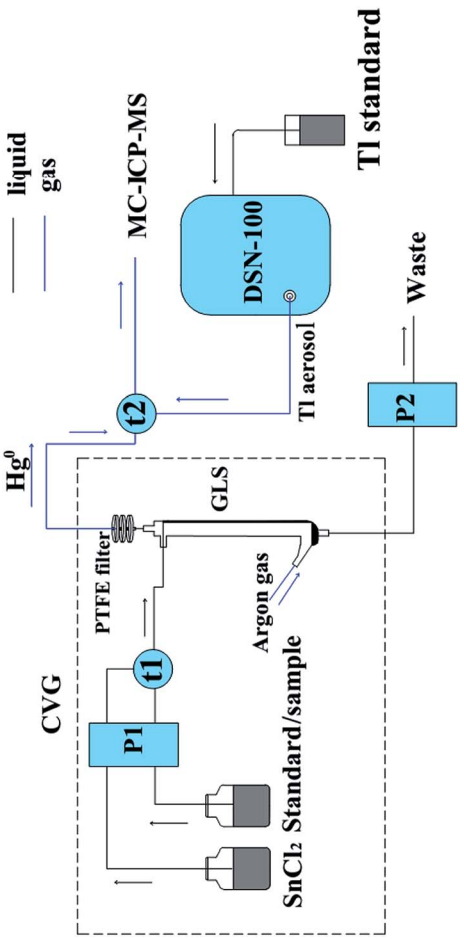

Fig. 1 Schematic of the introduction device (CVG: cold-vapor generator, GLS: gas–liquid separator, DSN-100: desolvating nebulizer, MC-ICP-MS: multi-collector inductively coupled plasma mass spectrometer, P1, P2: pump 1, pump 2, t1, t2: tee 1, tee 2).

(Baoding Longer Precision Pump Co., China.) were used to introduce standard/sample and reagents, and to remove waste from the GLS.

The DSN-100 was employed for the Tl introduction. Seven Faraday cups of the MC-ICP-MS were used to detect Hg and Tl isotope, in which, L6, L5, L4, L3, L2, L1, Ax and H1 were set for ^{198}Hg, ^{199}Hg, ^{200}Hg, ^{201}Hg, ^{202}Hg, ^{203}Tl, ^{204}Hg and ^{205}Tl. The concentration of ^{196}Hg was too low to be detected; the isotope was not used in the measurement.

The uptake rate of the Hg standard, sample and reagents was adjusted to 0.75 mL min^{-1}, and that of the Tl standard was 0.10 mL min^{-1}. Between standard and sample, the CVG and DSN-100 were rinsed with 3% (v/v) HNO_3 solution for 7 min until the signal intensity returned to the background level, typically between 10–30 mV.

A cold vapor atomic fluorescence spectrophotometer (Rayleigh Analytical Instrument Corp., China) was used for the analysis of total Hg.[30]

Reagents and solutions

All reagents were prepared in ultrapure water (18.00 MΩ cm) from a water purification system (Millipore, USA). HCl, HNO_3 and H_2SO_4 (Merck, Germany) of GR grade were used for vessel cleaning and reagent preparation. A 0.13 mol L^{-1} $SnCl_2 \cdot 2H_2O$ (Xilong Chemical Co. China) solution was prepared in 1.20 mol L^{-1} HCl. The $SnCl_2$ solution was purged prior to use with Hg-free Ar gas overnight to remove Hg. Bromine monochloride (BrCl) solution was made by dissolving 5.40 g of potassium bromide (Xilong Chemical Co. China) in 0.50 L of HCl with stirring for approximately 1 h in a fume hood, then slowly adding 7.60 g of potassium bromate (Xilong Chemical Co. China) with stirring for another hour. The $KMnO_4$ (Alfa Aesar, UK) solutions of 1.00–5.00 mmol L^{-1} were prepared in 0.50 mol L^{-1} H_2SO_4.[17,19,31] The Hg (NIST SRM 3133) and Tl (NIST SRM 997) standard solutions were purchased from the National Institute of Standards and Technology, USA, and their certified compositions were reported in earlier research.[32,37] The UM-Almadén in-house secondary standard was kindly provided by Dr Blum of the University of Michigan.[32]

Sample collection and preparation

Seawater samples were collected from a coal-fired power plant located near Xiamen western sea area, Fujian. The plant is equipped with a seawater flue gas desulfurization system. Five sampling sites were selected, including the inlet pool of fresh seawater (S1), the outlet of the desulfurization tower (S2), inside the aeration pool (S3 and S4) and the outlet of waste seawater (S5). Sampling and sample preparation were performed following the US EPA (1996) method. 5–10 L of seawater was collected and filtered through a 0.45 μm acetate cellulose membrane. The filtrate was stabilized in 0.5% (v/v) BrCl (US EPA, 1631).

Purge and trap preconcentration

The dissolved Hg in the spike samples and the seawater samples was preconcentrated with a purge and trap method. After the treatment, the Hg concentration in the trapping solution could be up to 3.00 ng mL^{-1}. The arrangement of the purge and trap method is schematically illustrated in Fig. 2. In Fig. 2a, within a 2 L purge bottle, the Hg^0 was purged with Ar gas at a flow rate of 300–400 mL min^{-1}, and then consequently trapped onto a series of Au columns (Au-1, Au-2, Au-3) containing gold-coated glass beads (Brooks Rand Lab, USA). A drying column filled with soda lime was inserted before the Au columns to protect the gold trap from moisture. As shown in Fig. 2b, the Au columns were then transferred to a thermal desorption device (D), and desorption was performed at 500 °C for several seconds to release Hg^0 in each column. The carrier gas at a flow rate of 20 mL min^{-1} sent the released Hg^0 to the trapping solution containing $KMnO_4$. Another Au column (Au-4) was placed at the outlet of the trapping bottle to trap Hg^0 residues, which could verify if Hg^0 was efficiently trapped in the $KMnO_4$ solution. Teflon tubing was used[28] as transfer lines in the purge and trap system.

Data analysis

Instrumental mass bias was monitored and corrected using the internal correction method and the standard-sample bracketing method.[33] The exponential mass fractionation law was applied as the internal correction method assuming a reference ^{205}Tl/^{203}Tl value of 2.38714 for the Tl internal standard. The Tl to Hg signal ratio was adjusted to 0.80–1.00.[32] The results of Hg isotopic measurements can be expressed as δ-values,[34] which represent the MDF of isotopes:

$$\delta^{xxx}\mathrm{Hg}\ (‰) = [(^{xxx}\mathrm{Hg}/^{198}\mathrm{Hg})_{\mathrm{sample}}/(^{xxx}\mathrm{Hg}/^{198}\mathrm{Hg})_{\mathrm{standard}} - 1] \times 1000 \quad (1)$$

where ^{xxx}Hg is ^{199}Hg, ^{200}Hg, ^{201}Hg and ^{202}Hg. The MIF of Hg isotopes was expressed as Δ^{xxx}Hg values, which can be calculated using the following equation:[31]

$$\Delta^{xxx}\mathrm{Hg} = \delta^{xxx}\mathrm{Hg} - (\delta^{202}\mathrm{Hg} \times \beta) \quad (2)$$

where the fractionation factor β is 0.2520, 0.5024 and 0.7520 for ^{199}Hg, ^{200}Hg and ^{201}Hg.

Results and discussion

Optimization of parameters for isotope measurement

Gas–liquid separators. The design of the modified CVG was focused on improving the Hg signal and simplifying the device. As a core part of the CVG, the GLS was designed to be tube-shape with a cylindrical chamber of 10 mm i.d. and 250–400 mm height. Diagrams of four home-made GLSs and the commercial one are shown in Fig. 3. In the four home-made GLSs, the main outlets at the top and at the bottom were the outlet of the carrier gas and waste, respectively. The side inlets near the top and near the bottom were the inlets for mix solution and carrier gas, respectively. The height of the GLS and the flow way of the carrier gas were different among the four GLSs. The height of GLS-1 and GLS-2 was 400 mm, GLS-3 was 300 mm, and GLS-4 was 250 mm. The carrier gas flowed horizontally into

GLS-1. There was a 45° angle between the bottom side inlet and the cylindrical chamber for GLS-2, GLS-3 and GLS-4. The commercial GLS is U-shaped and embedded with a frosted glass post, and the carrier gas flows horizontally into it.

The gas–liquid separation efficiency of the GLSs was the ratio of the amount of Hg^0 purged out by the carrier gas to the initial amount of Hg in the standard. When the mixed solutions of $SnCl_2$ and Hg standard were continuously pumped into the GLS, Hg^0 reduced from Hg^{2+} was purged and carried out by Ar gas. An Au blank column was installed on the top outlet of the GLS to trap Hg^0 for 20 s and then the amount of Hg^0 on the Au column was quantitatively analysed and considered as the amount of Hg^0 purged out by the carrier gas. As the initial amount of Hg in the standard solution was known, the separation efficiency of the GLS could be calculated. The measured efficiencies of the four GLSs were 101.1 ± 4.8% (SD, $n = 12$), which corresponded to the previous studies.[35,36]

The Hg concentration of 3.00 ng mL^{-1}, 100 integration cycles and 5 s per cycle were chosen as the conditions in the comparison test of the ^{202}Hg signal and standard error of $\delta^{202}Hg$ with the four modified GLSs. The ^{202}Hg signal was 2.86 ± 0.05 V for GLS-1, 2.88 ± 0.02 V for GLS-2, 2.87 ± 0.02 V for GLS-3, and 2.84 ± 0.04 V for GLS-4 (SD, $n = 3$). V stands for volts, the unit of the ^{202}Hg signal given by the MC-ICP-MS. No significant statistical differences were identified among the four GLSs. However, a relatively strong and steady signal was found in GLS-2 and GLS-3. The main reason could be that the angle between the gas inlet and the cylindrical chamber greatly improved the turbulent flow of the carrier gas, resulting in efficient purge[35] of Hg^0 from the mixed solution. The $\delta^{202}Hg$ values of GLS-2 (0.01 ± 0.03‰, 2SD, $n = 3$) and GLS-3 (−0.01 ± 0.03‰, 2SD, $n = 3$) were close to each other, but the larger dead volume in the higher cylindrical chamber of GLS-2 was inconvenient to use compared to GLS-3. Therefore, GLS-3 was considered to be the best one to use among the four.

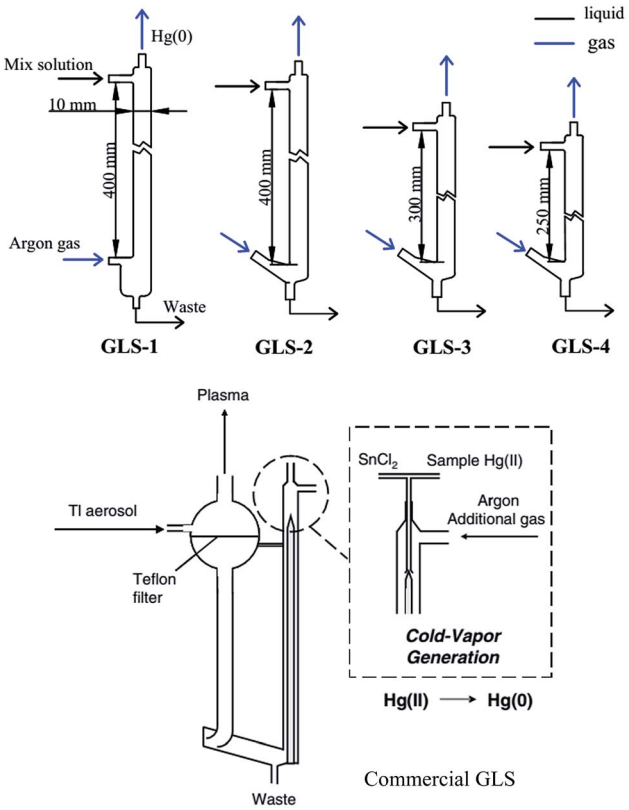

Fig. 3 Diagram of four GLS designs (GLS-1, GLS-2, GLS-3, GLS-4) and the commercial GLS.[23,37]

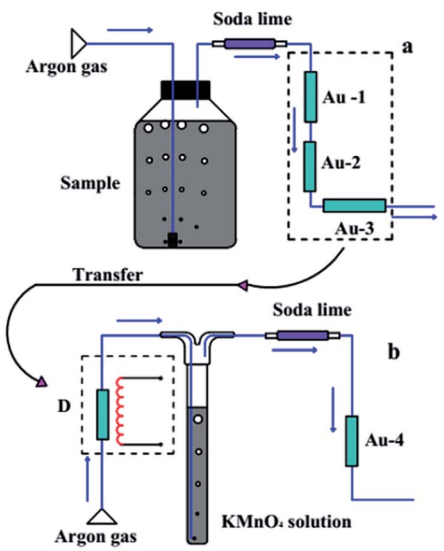

Fig. 2 The purge (a) and trap (b) method for dissolved Hg preconcentration (Au-1, Au-2 and Au-3: Au column 1, 2 and 3, Au-4: Au column for trapping Hg residues, D: thermal desorption device).

Compared with the commercial GLS, there were three major advantages in the modified GLSs. First, the dead volume was reduced, and the chamber could be washed more easily. Second, the carrier gas flowed from the bottom side inlet to the top of the GLS in an opposite direction to the mix solution, which provided turbulent flow of the carrier gas for rapid and efficient gas–liquid separation. Third, the modified introduction device consumed less carrier gas than the commercial one. The ^{202}Hg signal with a modified introduction device was 2.84–2.88 V at the Hg concentration of 3 ng mL^{-1}, while that with the commercial one was 0.60–1.32 V.[11,37] The Hg signal with a modified introduction device was twice that of the commercial one, showing a significant improvement in sensitivity for Hg isotopic analysis.

Data acquisition time. Data acquisition time was one of the key parameters in order to achieve good internal precision. 100 integration cycles was adopted in a single block using an Hg standard with concentration of 3.00 ng mL^{-1}. The internal precision was expressed as the standard error of data collected in a single block. By varying the integration time from 2 to 10 s per cycle, the total acquisition time was in the range 200 s to 17 min. As shown in Fig. 4a, an obvious improvement in the internal precision of $\delta^{202}Hg$ was found when the integration time per cycle was longer than 6 s. Thus 6 s was chosen as the integration time to obtain an internal precision of better than

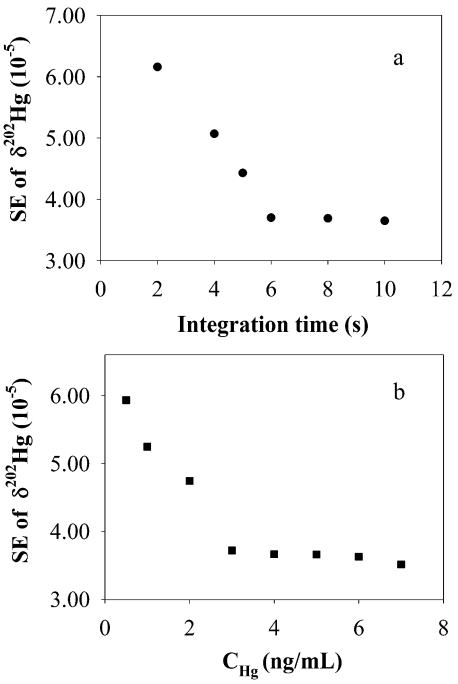

Fig. 4 Effect of integration time (a) and Hg concentration (b) on precision of δ^{202}Hg (SE: standard error).

0.04‰, and the total acquisition time was 10 min. A sample volume of 9.0 mL was needed for a single measurement.

Mercury concentration in samples. The mercury concentration in prepared samples was another factor affecting the internal precision. When the Hg concentration increased from 0.50 to 7.00 ng mL^{-1}, the internal precision of each measurement increased from 0.06 to 0.03‰ (Fig. 4b). A ^{202}Hg signal of approximately 2.80 V was achieved with the Hg concentration at 3 ng mL^{-1}, and the internal precision was better than 0.04‰, which was considered to be good enough for the analysis. Higher concentrations did not significantly improve internal precision, but increased the rinsing time and the risk of carry over between samples. Consequently, the Hg concentration of 3 ng mL^{-1} was required for isotopic measurement to obtain designed accuracy and reproducibility, the concentration was lower than earlier research.[10,11,17,23,37]

External precision and accuracy of long-term measurement. The Hg standards of NIST SRM 3133 and UM-Almadén were repeatedly measured to evaluate the external precision and accuracy of the proposed device. The data for NIST SRM 3133 were collected from 13 different measuring sessions over a period of a year. The external precision, also named as uncertainty, was expressed as twice the standard deviation (2SD) of the data in different measuring sessions. The external precision with the modified Hg introduction device was 0.05‰ for δ^{202}Hg, which was better than the reported studies.[10,22,26,38] The δ^{202}Hg was 0.00 ± 0.05‰ (2SD, n = 310), and Δ^{199}Hg was 0.00 ± 0.02‰ (2SD, n = 310). No MDF and MIF were found in the analysis process. In conclusion, the device is practical and reliable.

The UM-Almadén in-house secondary standard was analysed in seven different measuring sessions over seven months. The δ^{202}Hg values were −0.57 ± 0.10‰ (2SD, n = 49) without MIF, which fitted well with previous results.[32]

Optimization of parameters of the preconcentration system

Concentration of $KMnO_4$ solution. The concentration of $KMnO_4$ (1.00–5.00 mmol L^{-1}) in the trapping solution was tested for trapping a certain mass of Hg. The Hg recoveries with different $KMnO_4$ concentrations were in the range of 99.6–102.8% with Hg addition of 75 ng. These recoveries were comparable with a previous study,[17] where 25, 40 and 250 ng of Hg were spiked into a 1 L sample and sample recoveries were 74.0–97.0%. It was proved that concentrations of $KMnO_4$ ranging from 1.00 to 5.00 mmol L^{-1} were all suitable for trapping Hg^0. Among them, the solution of 2.00 mmol L^{-1} was chosen as the trapping solution due to its good recovery and SD. The Hg isotopic composition in 2.00 mmol L^{-1} $KMnO_4$ was 0.02 ± 0.04‰ (2SD, n = 3) for δ^{202}Hg, which was acceptable.

Flow rate of the purge gas. A flow rate of the purge gas ranging from 100 to 600 mL min^{-1} was optimized with the Hg concentration of 15 ng L^{-1}. If the gas flow rate was too low, Hg was hard to purge from the solution. On the other hand, if the flow rate was too high, it could be more difficult for Hg^0 to be absorbed on the Au columns (Fig. 2a, Au-1, Au-2, Au-3), and the Hg^0 could escape to the air. Fig. 5a shows the recoveries at different purge flow rates within 95.0–105.0% with a gas flow rate ranging from 100 to 600 mL min^{-1}. Compared with those with flow rates of 100–200 mL min^{-1}, the air bubbles from the purge were fine and abundant in the solution with the rate of 300–400 mL min^{-1}, which showed better results. On the other hand, the flow rate of 500–600 mL min^{-1} was too high.

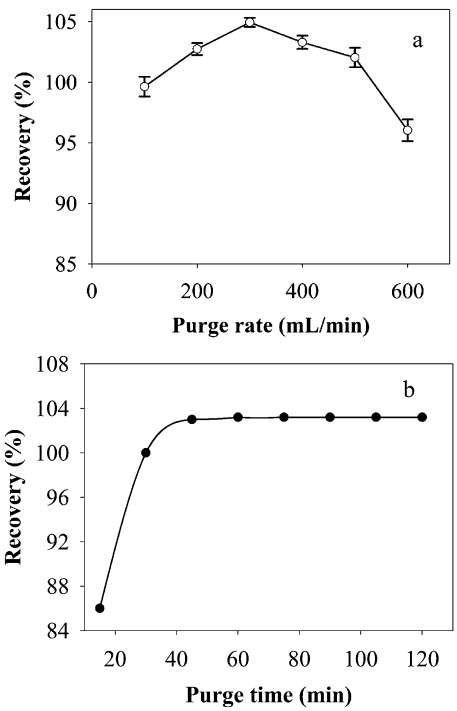

Fig. 5 Effect of purge flow rate (a) and purge time (b) on Hg recovery.

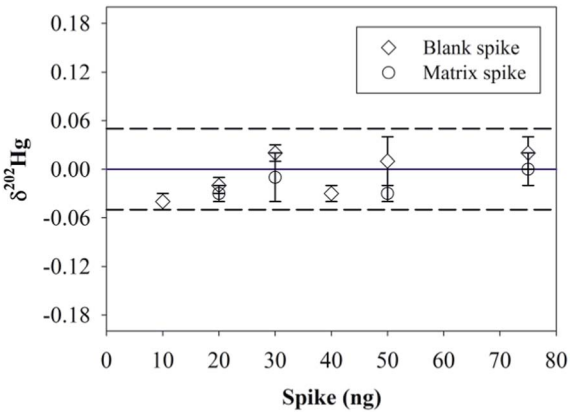

Fig. 6 δ^{202}Hg variation of the spike samples.

Therefore, 300 mL min^{-1} was employed as the gas flow rate for purge to obtain better reproducibility represented as SD, and finer air bubbles.

Purge time. A Hg concentration of 15 ng L^{-1} and a gas flow rate of 300 mL min^{-1} were chosen to study the influence of purge time on Hg recovery. As shown in Fig. 5b, the recovery greatly increased with purge time from 0 to 50 min, and then it slowly reached a plateau at about 103.0% after 60 min purge. Hence, 75 min was selected as the purge time.

Blank spike and matrix spike. In order to study the effect of a different matrix on the purge and trap method, ultrapure water and seawater collected from a coal-fired plant were selected to be the matrices for the blank spike and the matrix spike, respectively. Based on the concentration of the discharged waste seawater, the seawater samples were spiked with NIST SRM 3133 at different Hg masses of 20, 30, 50, and 75 ng. The Hg recoveries of the spike samples were within 95.0–105.0%, which proved that the spiked Hg was efficiently trapped in the $KMnO_4$ solution. The δ^{202}Hg values of the trapping solution after preconcentration are shown in Fig. 6. The δ^{202}Hg values were 0.00 ± 0.04‰ (2SD, n = 19) for the blank spike and −0.02 ± 0.04‰ (2SD, n = 12) for the matrix spike. After preconcentration, δ^{202}Hg variation in the trapping solution was very small compared with the composition of NIST SRM 3133.

In general, the modified device and proposed preconcentration method were reliable, and precise, and could be used to analyse the Hg isotopic composition of real samples.

Preconcentration of Hg from seawater. As previously mentioned, a sample of 9.0 mL 3 ng mL^{-1} was required for the isotopic measurement. Once the Hg concentration of seawater sample was less than 3 ng mL^{-1}, the preconcentration should be processed. The total Hg concentration of the seawater discharged from the coal-fired power plant was ranged between 5–100 ng L^{-1},[30] and the dissolved Hg concentration was less than 70 ng L^{-1}, thus 0.5–10.0 L seawater samples was needed for the preconcentration.

Table 1 lists the Hg recoveries and isotopic composition. The recovery was defined as the amount of Hg in the trapping solution to that of the seawater sample. The Hg recoveries from the seawater samples were within 95.0–104.0%.

Slightly negative MDF was observed (δ^{202}Hg = −0.23‰ to −0.02‰) in the seawater samples except for S2 (δ^{202}Hg = 0.12 ± 0.04‰, 2SD, n = 3). The δ^{202}Hg values were different from that of Arctic snow[19] and lake water.[27] The Hg isotopic composition of seawater differed greatly from that of fresh waters. The δ^{202}Hg value of S2 located at the outlet of the desulfurization tower was positive, which was different from that of the fresh seawater S1 (−0.10 ± 0.06‰, 2SD, n = 3), the result indicated that the heavier Hg isotopes were enriched in the seawater in the desulfurization tower. The physical and chemical process,[41] including evaporation, diffusion, redox and adsorption of Hg in the tower, could be the reason for the enrichment of heavier isotopes. As the heaviest isotope, the variation range of δ^{204}Hg value was the largest, from −0.76‰ to 0.36‰. The change of δ^{204}Hg value from fresh seawater to the desulfurization seawater was also positive, providing a useful and potential tracing parameter for Hg. The data of isotopic signature of dissolved Hg would be very helpful to explain the mechanism of sea–air exchange and deposition of Hg.

The seawater samples displayed significant MIF of odd isotope (Δ^{199}Hg = −0.09‰ to −0.16‰, Δ^{201}Hg = −0.11‰ to −0.22‰), the reason might be photo-reduction[4,39] volatilization[6] and other natural processes.[40] No MIF of ^{200}Hg was found in the seawater samples.

Conclusions

A modified introduction device and preconcentration method for the determination of the dissolved Hg isotopic composition of seawater were developed in the present study. The relevant parameters were optimized to achieve the best performance,

Table 1 Hg isotope compositions in seawater samples[a]

Sample	Dissolved total Hg (ng L^{-1})	Recovery (%, SD)	δ^{199}Hg (‰, 2SD)	δ^{200}Hg (‰, 2SD)	δ^{201}Hg (‰, 2SD)	δ^{202}Hg (‰, 2SD)	δ^{204}Hg (‰, 2SD)	Δ^{199}Hg (‰, 2SD)	Δ^{201}Hg (‰, 2SD)
S1 (n = 3)	20.54	98.4 ± 3.4	−0.14 ± 0.06	−0.03 ± 0.06	−0.18 ± 0.02	−0.10 ± 0.06	−0.19 ± 0.08	−0.12 ± 0.06	−0.11 ± 0.06
S2 (n = 3)	54.07	99.7 ± 2.5	−0.03 ± 0.04	0.09 ± 0.04	−0.05 ± 0.04	0.12 ± 0.04	0.36 ± 0.02	−0.11 ± 0.04	−0.14 ± 0.08
S3 (n = 3)	49.68	97.5 ± 2.1	−0.19 ± 0.04	−0.14 ± 0.10	−0.32 ± 0.04	−0.20 ± 0.06	−0.75 ± 0.04	−0.14 ± 0.04	−0.17 ± 0.08
S4 (n = 3)	66.30	100.8 ± 3.5	−0.18 ± 0.04	−0.06 ± 0.04	−0.25 ± 0.04	−0.18 ± 0.06	−0.31 ± 0.08	−0.13 ± 0.06	−0.11 ± 0.06
S5 (n = 3)	3.66	98.8 ± 3.0	−0.14 ± 0.04	−0.02 ± 0.06	−0.10 ± 0.02	−0.05 ± 0.06	−0.00 ± 0.10	0.14 ± 0.02	−0.11 ± 0.06

[a] Hg isotope analytical uncertainties are 2 times standard deviations (2 SD), n: number of samples.

and the precision and accuracy indicated that the proposed method was stable and reliable. The proposed method was applied to study the MDF and MIF in desulfurized seawater samples. The Hg isotope composition of the waste seawater at the outlet of the desulfurization tower showed a different isotope compared with other seawater samples, which could be caused by evaporation, diffusion, redox and adsorption of Hg in the tower. The isotopic signature of dissolved Hg could provide useful information for explanation of the mechanism of sea–air exchange and deposition of Hg.

Acknowledgements

This research was financed by the Natural Science Foundation of China (21277112). The authors would like to thank Professor John Hodgkiss for helping to prepare this manuscript. The authors also thank Joel D. Blum for providing the UM-Almadén in-house secondary standard.

Notes and references

1 L. Si and P. A. Ariya, *Environ. Sci. Technol.*, 2008, **42**, 5150–5155.
2 W. F. Fitzgerald, C. H. Lamborg and C. R. Hammerschmidt, *Chem. Rev.*, 2007, **107**, 641–662.
3 R. P. Mason and G. R. Sheu, *Global Biogeochem. Cycles*, 2002, **16**, 1093.
4 W. Zheng and H. Hintelmann, *Geochim. Cosmochim. Acta*, 2009, **73**, 6704–6715.
5 N. Estrade, J. Carignan, J. E. Sonke and O. F. X. Donard, *Geochim. Cosmochim. Acta*, 2009, **73**, 2693–2711.
6 W. Zheng, D. Foucher and H. Hintelmann, *J. Anal. At. Spectrom.*, 2007, **22**, 1097.
7 K. Kritee, J. D. Blum and T. Barkay, *Environ. Sci. Technol.*, 2008, **42**, 9171–9177.
8 K. Kritee, J. D. Blum, M. W. Johnson, B. A. Bergquist and T. Barkay, *Environ. Sci. Technol.*, 2007, **41**, 1889–1895.
9 A. Biswas, J. D. Blum, B. A. Bergquist, G. J. Keeler and Z. Q. Xie, *Environ. Sci. Technol.*, 2008, **42**, 8303–8309.
10 D. Foucher, H. Hintelmann, T. A. Al and K. T. Macquarrie, *Chem. Geol.*, 2013, **336**, 87–95.
11 X. B. Feng, D. Foucher, H. Hintelmann, H. Y. Yan, T. Y. He and G. L. Qiu, *Environ. Sci. Technol.*, 2010, **44**, 3363–3368.
12 C. N. Smith, S. E. Kesler, J. D. Blum and J. J. Rytuba, *Earth Planet. Sci. Lett.*, 2008, **269**, 399–407.
13 D. Foucher and H. Hintelmann, *Environ. Sci. Technol.*, 2009, **43**, 33–39.
14 D. R. Thompson, S. Bearhop, J. R. Speakman and R. W. Furness, *Environ. Pollut.*, 1998, **101**, 193–200.
15 S. Onsanit, M. Chen, C. H. Ke and W. X. Wang, *J. Hazard. Mater.*, 2012, **203–204**, 13–21.
16 R. S. Yin, X. B. Feng and B. Meng, *Environ. Sci. Technol.*, 2013, **47**, 2238–2245.
17 L. E. Gratz, G. J. Keeler, J. D. Blum and L. S. Sherman, *Environ. Sci. Technol.*, 2010, **44**, 7764–7770.
18 W. Zheng and H. Hintelmann, *Geochim. Cosmochim. Acta*, 2009, **73**, 6704–6715.
19 L. S. Sherman, J. D. Blum, K. P. Johnson, G. J. Keeler, J. A. Barres and T. A. Douglas, *Nat. Geosci.*, 2010, **3**, 173–177.
20 J. B. Chen, H. Hintelmann, X. B. Feng and B. Dimock, *Geochim. Cosmochim. Acta*, 2012, **90**, 33–46.
21 Š. Marko, H. Holger and D. Dimock, *Analytica Chimica Acta*, 2014, **851**, 57–63.
22 R. S. Yin, X. B. Feng, J. X. Wang, Z. D. Bao, B. Yu and J. B. Chen, *Chem. Geol.*, 2013, **336**, 80–86.
23 D. Foucher and H. Hintelmann, *Anal. Bioanal. Chem.*, 2006, **384**, 1470–1478.
24 L. S. Sherman, J. D. Blum, D. K. Nordstrom, R. B. McCleskey, T. Barkay and C. Vetriani, *Earth Planet. Sci. Lett.*, 2009, **279**, 86–96.
25 N. S. Bloom and E. A. Crecelius, *Mar. Chem.*, 1983, **14**, 49–59.
26 L. S. Sherman, J. D. Blum, G. J. Keeler, J. D. Demers and J. T. Dvonch, *Environ. Sci. Technol.*, 2012, **46**, 382–390.
27 J. B. Chen, H. Hintelmann and B. Dimock, *J. Anal. At. Spectrom.*, 2010, **25**, 1402–1409.
28 G. A. Gill and W. F. Fitzgerald, *Mar. Chem.*, 1987, **20**, 227–243.
29 M. Wojciechowski, A. Krata and E. Bulska, *Chem. Anal.*, 2008, **53**, 797–808.
30 X. Y. Liu, L. M. Sun, D. X. Yuan, L. Q. Yin, J. Y. Chen, Y. X. Liu, C. Y. Liu, Y. Liang and F. F. Lin, *Environ. Sci. Pollut. Res.*, 2011, **18**, 1324–1332.
31 W. Zheng and H. Hintelmann, *J. Phys. Chem. A*, 2010, **114**, 4238–4245.
32 J. D. Blum and B. A. Bergquist, *Anal. Bioanal. Chem.*, 2007, **388**, 353–359.
33 J. E Sonke, J. Schäfer, J. Chmeleff, S. Audry, G. Blanc and B. Dupré, *Chem. Geol.*, 2010, **279**, 90–100.
34 B. A. Bergquist and J. D. Blum, *Elements*, 2009, **5**, 353–357.
35 C. P. Hanna, P. E. Haigh, J. F. Tyson and S. McIntosh, *J. Anal. At. Spectrom.*, 1993, **8**, 585–590.
36 B. Klaue and J. D. Blum, *Anal. Chem.*, 1999, **71**, 1408–1414.
37 R. S. Yin, X. B. Feng, D. Foucher, W. F. Shi, Z. Q. Zhao and J. Wang, *Chin. J. Anal. Chem.*, 2010, **38**, 929–934.
38 R. S. Yin, X. B. Feng, J. X. Wang, P. Li, J. L. Liu, Y. Zhang, J. B. Chen, L. R. Zheng and T. D. Hu, *Chem. Geol.*, 2013, **336**, 72–79.
39 B. A. Bergquist and J. D. Blum, *Science*, 2007, **318**, 417–420.
40 K. Kritee, J. D. Blum, J. R. Reinfelder and T. Barkay, *Chem. Geol.*, 2013, **336**, 13–25.
41 R. Y. Sun, L. E. Heimbürger, J. E. Sonke, G. J. Liu, D. Amouroux and S. Berail, *Chem. Geol.*, 2013, **336**, 103–111.